Review Article

Response assessment and surveillance following stereotactic ablative radiotherapy for lung cancer

Dominique Mathieu, Houda Bahig

Centre hospitalier de l'Université de Montréal, Montréal, Quebec, Canada

Contributions: (I) Conception and design: None; (II) Administrative support: None; (III) Provision of study material or patients: None; (IV) Collection and assembly of data: None; (V) Data analysis and interpretation: None; (VI) Manuscript writing: All authors; (VII) Final approval of manuscript: All authors.

Correspondence to: Houda Bahig, MD, PhD. Centre hospitalier de l'Université de Montreal, Montréal, Quebec, Canada.
Email: houda.bahig.chum@ssss.gouv.qc.ca.

Abstract: Lung stereotactic ablative radiotherapy (SABR) is almost invariably associated with radiation-induced parenchymal injury within 3 years of treatment completion. While distinguishing normal fibrotic changes from local recurrence is challenging, accurate detection of local relapse has become increasingly crucial in the context of rapidly growing SABR patients' population and multiplying salvage therapy options. Knowledge of the natural history of radiation-induced lung injury as well as recognition of the risk factors associated with recurrence are essential to assist timely diagnosis of recurrence while avoiding unnecessary investigations. In this review, we discuss the patterns of recurrence after SABR, the expected post-treatment radiological changes as well as the prevailing and evolving strategies to differentiate recurrence from radiation-induced lung injury. The limitations of the current response assessment methods and the promising avenues of functional imaging and radiomics are discussed. Finally, current general consensus guidelines for surveillance post-SABR for early-stage non-small cell lung cancer are summarized.

Keywords: Recurrence; surveillance; stereotactic ablative radiotherapy (SABR); radiation induced lung injury; imaging changes

Received: 24 December 2018; Accepted: 21 March 2019; published: 25 April 2019.
doi: 10.21037/tro.2019.03.05
View this article at: http://dx.doi.org/10.21037/tro.2019.03.05

Introduction

Surveillance after stereotactic ablative radiotherapy (SABR) is essential for the assessment of primary tumor response, the early detection of locoregional and distant recurrences, and the diagnosis of second primary lung cancer (SPLC). Radiologically, distinguishing local recurrence from radiation-induced changes is challenging as intra-lesional and peri-tumoral parenchymal injury can frequently mimic tumor progression. A proper understanding of the normal tissue changes expected on surveillance imaging after SABR is critical to avoid unnecessary investigations and facilitate timely diagnosis of recurrence. This is particularly important in the context of the expanding role of SABR in fitter patients that could be eligible to aggressive salvage (1), the growing role of SABR in the era of lung cancer screening programs leading to detection of early stage disease (2), and the favourable outcomes shown with various salvage strategies, including surgery, re-irradiation or systemic therapies (3-7). In this review, we will discuss the normal radiological changes expected after SABR, the current and evolving strategies to distinguish recurrence from lung parenchymal injury, as well as the general consensus for surveillance schedule in patients with early-stage non-small cell lung cancer (ES-NSCLC) treated with SABR.

Pattern of recurrence after SABR

The delivery of targeted, hypofractionated radiotherapy

Table 1 Tumor and treatment related factors associated with local recurrence after lung SABR

Category	Factor
Clinical	T-stage: T2 *vs.* T1 (11,12)
	Tumor size/volume:
	Larger GTV (3,13,14)
	GTV ≥8.3 cm^3 (15)
	Histologic subtype: squamous cell carcinoma (16,17)
	PET uptake value:
	Pre-treatment SUV_{max} >3 (18)
	Pre-treatment SUV_{max} ≥6 (19)
	Residual SUV_{max} 12 weeks post SABR ≥5 (20)
Treatment	Dosimetry:
	BED_{10} <100 Gy (21)
	PTV95 BED_{10} ≤86 Gy (15)
	PTVmean BED_{10} ≤130 Gy (15)
	Treatment time: duration ≥11 days (22)
	Dose calculation algorithm: pencil beam *vs.* collapsed cone convolution (23)

SABR, stereotactic ablative radiotherapy; PET, positron-emission tomography; BED, biological equivalent dose; GTV, gross tumor volume; PTV, planning target volume; SUV, standardized uptake value; BED, biologically effective dose.

for ablation of early-stage lung cancer provides excellent biological efficacy, with 5-year local control around 90% (6,8-10). Across studies, rates of local failure have varied between 7–20%, based on whether local recurrence was defined as progression within or adjacent to the treated volume (6) or progression within the involved lobe (10), and whether pathological confirmation was obtained. Local recurrence can be further classified as in-field (within the target volume), marginal (around the target volume) or within the involved lung lobe (10). As outlined in *Table 1*, several factors have been associated with local recurrence and recognition of these factors can provide insight for better interpretation of radiological changes and optimization of surveillance strategies. Tumor factors include higher T-stage and tumor size (10), squamous histologic subtype (16,24,25) and high pre-treatment standardized uptake value (SUV) on positron-emission tomography (PET) (19). Treatment factors comprise lower biologically effective dose, planning target volume dose, fractionation and possibly differences in delivery techniques (23,24,26). Despite high local control rates, regional and distant failures are common, with rates of 13% and 20% at 5-year, respectively (9). While the vast majority of recurrences are diagnosed within the first 2 years after SABR, late recurrences can occur up to 5 years post-treatment (6,9,27). In addition, the cumulative rate of SPLC at 5-year post-SABR is 18% (6,10,11); many of these SPLC can be addressed with further ablative treatment when caught early on surveillance imaging.

Lung injury after SABR

The term radiation induced lung injury involves a spectrum of post-treatment parenchymal changes, from radiation pneumonitis (RP) occurring within 6 months of SABR to radiation fibrosis occurring after 6 months (28). The median time to appearance of radiological lung injury is 17 weeks; however, up to 1 in 4 patients will show the first signs of injury as late as 1 year post-treatment (29). RP can be subclinical and diagnosed radiologically, but can also lead to life-threatening clinical RP (30). As many patients with lung cancer suffer from underlying lung disease associated with tobacco smoking, diagnosis of clinical RP is often challenging due to confounding differential diagnosis such as chronic obstructive lung disease exacerbation, interstitial lung disease exacerbation, disease progression or pneumonia (31,32). Clinical RP is characterized by dyspnea, cough, low-grade fever that may require steroid treatment, hospitalisation and in rare instances, respiratory failure that could lead to death (30). A recent pooled analysis from 88 studies showed that clinical RP after SABR is rare, with 9% rate of symptomatic RP (grade ≥2) and less than 2% rate of severe RP requiring oxygen therapy (grade ≥3) (33). However, emerging data suggest that certain subgroups may be at higher risk of developing severe clinical RP post-SABR, including patients with large tumors beyond 5 cm (34,35) and patients with underlying interstitial lung disease (36). On the other hand, in a study analyzing acute radiological injury post-SABR, 54% of patients showed signs of radiological RP on computed tomography (CT) imaging following treatment (37). *Table 2* summarizes the main tumor and dosimetric factors that have been associated with radiation-induced lung injury in the literature (33-35,38,43,44). Acute radiological lung injury after SABR is described based on an adapted scoring system previously established

Table 2 Risks factors associated with radiation-induced lung toxicity

Category	Factor
Patients	Older age (33)
	Pre-existing interstitial lung disease (36,38,39)
	Biochemical markers (40):
	Serum Krebs von den Lungen-6 (KL-6)
	Serum surfactant protein-D (SP-D)
Tumor	T-stage: T2 *vs.* T1 (33)
	Tumor size:
	>5 cm (34)
	Larger tumor diameter (33)
	Larger GTV volume (14,41)
Treatment	Previous radiation (42)
Dosimetric	MLD to whole lung (33)
	V20 to whole lung (33)
	V5 to whole lung: V5 >37% (35)
	V5 to contralateral lung: V5 >26% (35)
	Larger PTV (41)

MLD, mean lung dose; V5, volume of lung receiving at least 5 Gy; V20, volume of lung receiving at least 20 Gy; GTV, gross tumor volume; PTV, planning target volume.

for conventional radiotherapy including diffuse (more than 5 cm) and patchy (less than 5 cm) consolidation, diffuse and patchy ground glass opacities or no evidence of increased density (37). Patchy consolidation (24%) and diffuse consolidation (16%) form the most commonly observed parenchymal changes.

Late fibrotic changes occur in most patients and typically appear as an area of increased density in the high-dose region, therefore often conforming to the shape of the initial tumor (28,29). At the histological level, fibrosis is characterized by proliferation of atypical pneumocytes, interstitial elastofibrosis and vascular thickening (45). When present on CT, fibrosis can be classified into three categories: modified conventional pattern (involving consolidation, volume loss, and bronchiectasis), scar-like (linear opacity within the tumor vicinity and volume loss) and mass-like (well-circumscribed focal consolidation surrounding the tumor region) (29,46,47). In a previous study looking at late post-SABR changes, the modified conventional, scar-like and mass-like patterns of fibrosis occurred in 71%, 11% and 7% of patients respectively, while the remaining patients showed no evidence of increasing density. Fibrotic changes have been shown to persist and even sometimes continue to evolve beyond 2 years post-SABR (29). The pattern and severity of fibrosis have been shown to vary based on factors such as dose and fractionation, treatment technique and tumor volume (37,48). Among the radiological patterns of late radiation induced changes, perhaps the most challenging is the mass-like fibrosis, which can frequently be confounded with tumor progression (29,49,50). As opposed to local recurrence, mass-like fibrosis frequently remains stable over time, but progression of the fibrotic pattern over time can be observed, further complicating distinction from tumor recurrence (29).

Strategies for distinguishing lung injury from recurrence

In view of their similar morphology and temporal course, radiation-induced changes and local recurrence can be difficult to differentiate (*Figures 1,2*) (28,51,52). Failure of timely detection of local recurrence could potentially jeopardize a chance of cure from salvage treatment. Although generally limited to small series and highly selected patients, salvage post-SABR has shown encouraging outcomes with 5-year overall survival reaching 80% (53,54). On the other hand, as reported in several case series of patients who underwent salvage resection and were found to have benign fibrosis (50,55,56), misclassification of radiation induced injury as local recurrence can lead to futile investigations with unnecessary risks and costs. The Response Evaluation Criteria for in Solid Tumors (RECIST) version 1.1, which relies on tumor dimensions assessed on anatomical imaging, remains the most commonly used system for tumor response assessment (57). However, given the expected radiological changes post-treatment, there is general agreement that these criteria are not well suited for response assessment post-SABR. In fact, the poor performance of tumor dimension changes as a predictor of local recurrence within 6 months of SABR was previously shown (58-60). Currently, a diagnosis of local recurrence post-lung SABR is generally based on radiological findings on serial CT, in combination with hypermetabolism on 18-fluoro-2-deoxy-D-glucose (FDG)-PET and pathological confirmation whenever possible.

Several high-risk CT features predictive of local recurrence were previously identified in a systemic review by Huang

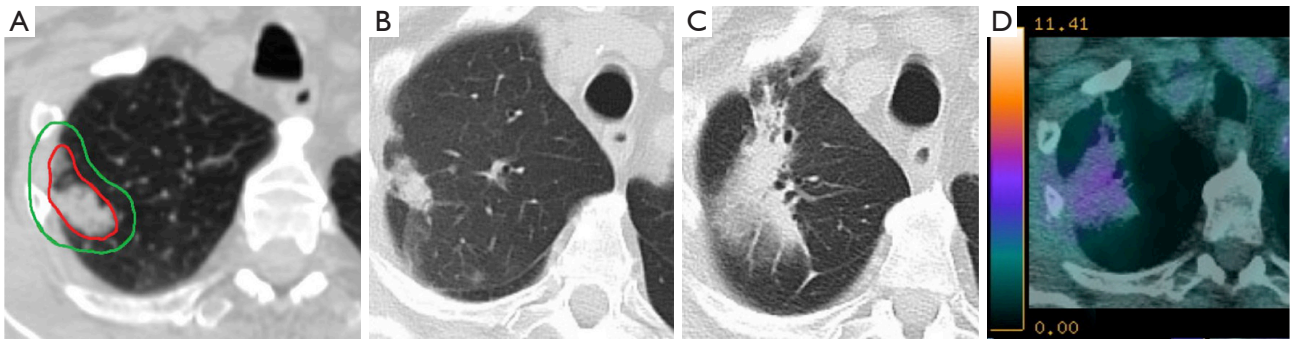

Figure 1 Serial CT scans and FDG-PET/CT from a patient with fibrotic radiation-induced changes. An 81-year-old man treated with robotic SABR for a T2bN0 adenocarcinoma of the right upper lobe to a dose of 60 Gy in 5 fractions; the patient developed late radiation fibrosis. SUV_{max} from FDG-PET at 4 years post-SABR was 0.6. Sequential imaging shows progressive installation of ground glass opacities and consolidation: (A) planning CT; (B) CT at 3 months; (C) CT at 4 years; (D) FDG-PET/CT at 4 years. Red and green contours represent respectively the gross tumor volume and planning target volume on the planning CT image. CT, computed tomography; FDG-PET, 18-fluoro-2-deoxy-glucose positron-emission tomography; SABR, stereotactic ablative radiotherapy; SUV, standardized uptake value; SUV_{max}, maximum SUV.

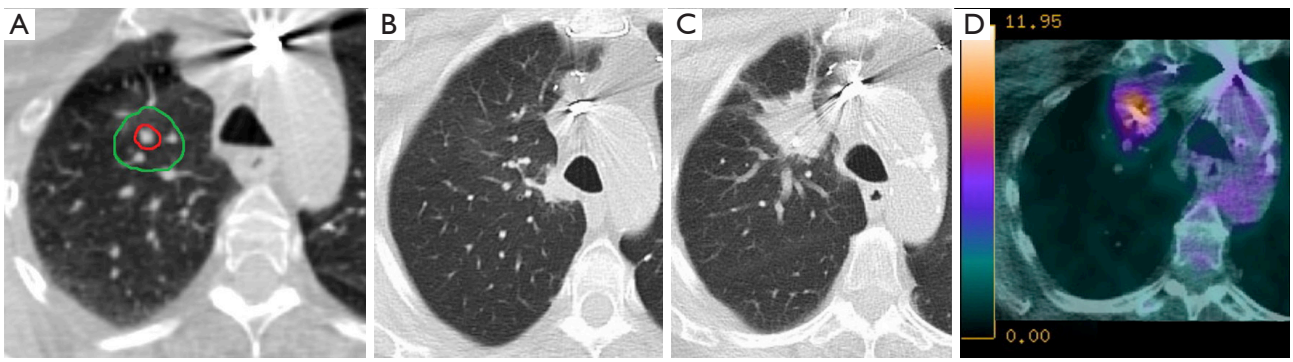

Figure 2 Serial CT scans and FDG-PET/CT from a patient with pathologically proven local recurrence. A 68-year-old woman treated with robotic SABR for a T1aN0 adenocarcinoma of the right upper lobe to a dose of 60 Gy in 3 fractions. She developed biopsy-proven local recurrence 3 years post treatment, with SUV_{max} of 4.2 on FDG-PET. Sequential imaging shows installation of a mass-like consolidation: (A) planning CT; (B) CT at 6 months; (C) CT at 3 years; (D) FDG-PET/CT at 3 years. Red and green contours represent respectively the gross tumor volume and planning target volume on the planning CT image. Several high-risk CT features can be seen, notably sequential enlargement, enlarging opacity after 12 months, craniocaudal growth and bulging margin. CT, computed tomography; FDG-PET, 18-fluoro-2-deoxy-glucose positron-emission tomography; SABR, stereotactic ablative radiotherapy; SUV, standardized uptake value; SUV_{max}, maximum SUV.

et al. (28); these features included: (I) enlarging opacity at the tumor site, (II) serially enlarging opacity, (III) loss of linear margin, (IV) convex bulging margin, (V) loss of air bronchograms, and (VI) enlarging opacity after 12 months (28). These criteria, along with the additional feature of craniocaudal growth ≥5 mm or ≥20%, were later validated in a matched cohort of 36 patients, including 12 patients with pathological proof of recurrence (61). In the latter study, an enlarging opacity after 12 months and craniocaudal growth were found to be the best predictors of recurrence. Furthermore, the presence of ≥3 high-risk CT features was found to have a sensitivity and specificity for local recurrence beyond 90%. These high-risk CT features were independently validated in another cohort of biopsy-proven cases of recurrence, which found this time that bulging margin, loss of linear margin and craniocaudal

growth were the strongest features associated with local recurrence (62).

There remains controversy around the diagnostic performance of these high-risk CT features, as findings across studies have not been unanimous. In fact, in a recent study from Ronden *et al.* (63), up to half of the patients without locally recurrent disease had developed high-risk features, and the presence of ≥3 high-risk CT features was observed in up to 25% of patients without recurrence. These conflicting findings, along with the inconsistent presence of pathological confirmation of recurrence across studies and the generally small cohorts of patients in studies investigating CT-based radiological changes, constitute limitations. However, a recent expert consensus recommended that until better methods emerge, the following CT features should raise suspicion for local recurrence: infiltration into adjacent structures, bulging margins, sustained growth, loss of air bronchograms, as well as mass-like, spherical and craniocaudal enlargement (64). It was also recommended that the number of features should be used to classify patients as being at low, intermediate, or high-risk of recurrence (64).

Functional imaging

The search for optimal imaging biomarkers for the effective diagnosis of local recurrence is an active area of investigation. In contrast to simple anatomic imaging, the use of functional imaging holds the promise of further characterizing tumors activity and aggressiveness by providing information regarding tumor glucose uptake, perfusion, hypoxia and proliferation.

FDG-PET is a functional imaging that has largely been integrated into routine clinical practice in patients presenting findings suspicious of recurrence on CT imaging. Due to the risk of false-positive uptake from RP, FDG-PET for investigation of local recurrence has increased specificity when obtained >6 months post-SABR (65,66); however, it should be stressed that inflammatory FDG avidity can persist beyond 12 months post-SABR (61). Given the conflicting findings in the literature, the optimal maximum SUV (SUV_{max}) threshold associated with local recurrence remains uncertain. Several studies support that a post-SABR SUV_{max} ≥5.0, or greater than the pre-treatment SUV_{max}, are the most sensitive findings of local recurrence (20,28,67). In a study including 132 patients with ES-NSCLC treated with SABR and followed with serial FDG-PET, SUV_{max} ≥5.0 after 3–6 months post-treatment had a positive predictive value of recurrence of 83% (68,69). In another study including 17 local recurrences (not all pathologically proven), SUV_{max} cutoffs of 3.2 and 4.2 on early and delayed acquisitions had a sensitivity and specificity for recurrence of 100% and 96–98%, respectively (66). However, FDG-PET values are subject to significant variation due to lack of protocol standardization across institutions, differences in timing of acquisition and quantity of injected FDG, as well as patient's related factors such as size or weight (70,71). Hypoxia PET tracers such as ^{18}F-fluoromisonidazole (F-MISO) have been reported pre-clinically for assessment of response after lung SABR in mice (72) but future studies are needed to define their clinical utility.

Lung magnetic resonance imaging (MRI) has historically been of limited use due to the issues of respiratory motion and low tissue density of the parenchyma, inducing signal-to-noise ratio reduction and magnetic susceptibility effects. In recent years, technology enhancements have allowed faster acquisition times and improved respiratory-gating techniques, which have resulted in better quality of lung MRI (73). The use of functional MRI, including diffusion weighted diffusion-weighted MRI (DW-MRI) to quantify cellular density within the tumoral region (74,75) and dynamic contrast-enhanced (DCE) to measure perfusion (76-78) are promising avenues for response assessment. In one study, DW-MRI was found to be an early predictor of treatment response after lung SABR, with significantly lower apparent diffusion coefficient values at 3 and 6 months in patients eventually developing local recurrence (74). Similarly, preclinical work support that hypofractionated radiotherapy to the lungs induces important vascular damage within the tumor that could be assessed with perfusion imaging such as DCE-MRI (79). Further work will help define the role of functional MRI for surveillance after lung SABR.

Radiomics

Radiomics is an emerging field involving the extraction of quantitative data from imaging using advanced image analysis (80,81). To undertake radiomics analyses, a region of interest is defined, from which a series of radiomic image features can be calculated (82). Such features include first-order statistics based on the distribution of the intensity histogram (mean, median and standard deviation), and second-order features that take into account the neighbouring relationships of voxels within the region of interest. Radiomics-based quantification of lung density for assessment of SABR-induced lung damage

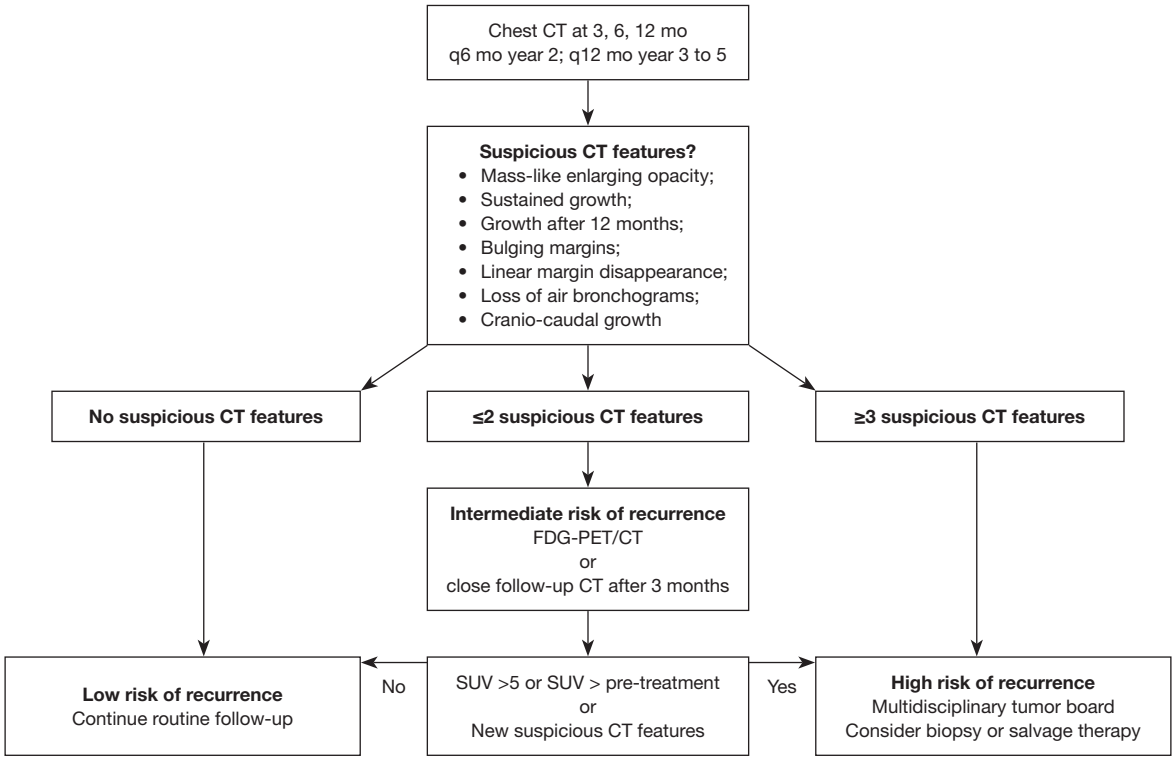

Figure 3 Schematic summary of the recommended surveillance after lung SABR based on the presence of high-risk CT features suspicious of local recurrence. CT, computed tomography; FDG-PET, 18-fluoro-2-deoxy-glucose positron-emission tomography; SUV, standardized uptake value; SBAR, stereotactic ablative radiotherapy.

has been investigated in several studies (83-85). Based on a dataset of 45 patients, a radiomic signature consisting of five image features could predict recurrence within 6 months post-SABR with a false-positive rate of 24% and a false-negative rate of 23% (60). The latter study showed that computer-aided texture analysis allowed earlier detection of recurrence post-SABR compared to physician-based scoring of high-risk features on CT. Another study by Fave *et al.* showed promising incorporation of radiomics on CT immediately at the end of treatment, to stratify patients into low *vs.* high risk of local relapse (86). Although the field of radiomics remains at its early stage, these findings suggest a promising role of texture analysis for early diagnosis and optimal therapeutic decision in patients treated with lung SABR.

Recommended surveillance schedule after lung SABR

Many guidelines, including those from the National Comprehensive Cancer Network (87) and the American Association of Thoracic Surgery (88), recommend follow-up CT examinations every 6 months for at least 2–4 years, followed by annual follow-up CT examinations. In a recent expert consensus from an International Delphi Consensus Study, there was general agreement that patients should be followed with routine CT post-SABR at 3, 6, and 12 months in year 1, every 6 months in year 2 and annually in years 3 through 5, and that an FDG-PET should obtained in case of suspicion of local recurrence (64). Although the exact frequency and duration of follow-up can be left at the discretion of the treating physician, more rigorous follow-up and lower threshold to trigger investigations is justified in patients at higher risk of local recurrence, including those with larger tumors, suboptimal radiation dose, or high pre-treatment SUV_{max} (12,19,89). Although no definite guidelines exist for follow-up of patients with suspected recurrence, one suggested algorithm proposes that patients at low-risk (with no suspicious CT features) could have routine follow-up, patients at intermediate-risk (with ≤2 suspicious CT features) could benefit from FDG-PET/CT or closer follow-up CT after 3 months, while patients at

high-risk (with ≥3 suspicious features on CT) could proceed to a biopsy or salvage therapy after careful evaluation and discussion in a multidisciplinary tumor board (61). A schematic summary of the recommended surveillance after lung SABR is presented in *Figure 3*.

Conclusions

Although lung SABR yields excellent tumor control outcomes, local relapse does occur in about 1 in 10 patients and is often difficult to distinguish from radiation induced lung injury such as pneumonitis or late fibrotic changes. Several tumor and treatment related factors are predictive of local control including gross tumor volume, histologic subtype, pre-treatment SUV and biologically effective dose. Surveillance with serial CT acquisition over the 5 years following treatment is recommended in ES-NSCLC patients treated with SABR. Usage of systematic imaging CT features to detect high-risk features of local recurrence such as bulging margins, sustained growth and craniocaudal growth can help identify patients that could benefit from further investigations, including functional FDG-PET imaging, biopsy or even salvage treatment. In the future, quantitative functional imaging and radiomics may help further refine post-SABR tumor response assessment.

Acknowledgments

Funding: None.

Footnote

Conflicts of Interest: H Bahig received a research grant from Varian Medical Systems, unrelated to current work. D Mathieu has no conflicts of interest to declare.

Ethical Statement: The authors are accountable for all aspects of the work in ensuring that questions related to the accuracy or integrity of any part of the work are appropriately investigated and resolved.

References

1. Chang JY, Senan S, Paul MA, et al. Stereotactic ablative radiotherapy versus lobectomy for operable stage I non-small-cell lung cancer: a pooled analysis of two randomised trials. Lancet Oncol 2015;16:630-7.
2. Aberle DR, Adams AM, Berg CD, et al. Reduced lung-cancer mortality with low-dose computed tomographic screening. N Engl J Med 2011;365:395-409.
3. Allibhai Z, Cho BC, Taremi M, et al. Surgical salvage following stereotactic body radiotherapy for early-stage NSCLC. Eur Respir J 2012;39:1039-42.
4. Trakul N, Harris JP, Le QT, et al. Stereotactic ablative radiotherapy for reirradiation of locally recurrent lung tumors. J Thorac Oncol 2012;7:1462-5.
5. Carbone DP, Reck M, Paz-Ares L, et al. First-Line Nivolumab in Stage IV or Recurrent Non-Small-Cell Lung Cancer. N Engl J Med 2017;376:2415-26.
6. Verstegen NE, Lagerwaard FJ, Hashemi SM, et al. Patterns of Disease Recurrence after SABR for Early Stage Non-Small-Cell Lung Cancer: Optimizing Follow-Up Schedules for Salvage Therapy. J Thorac Oncol 2015;10:1195-200.
7. Neri S, Takahashi Y, Terashi T, et al. Surgical treatment of local recurrence after stereotactic body radiotherapy for primary and metastatic lung cancers. J Thorac Oncol 2010;5:2003-7.
8. Soldà F, Lodge M, Ashley S, et al. Stereotactic radiotherapy (SABR) for the treatment of primary non-small cell lung cancer; systematic review and comparison with a surgical cohort. Radiother Oncol 2013;109:1-7.
9. Senthi S, Lagerwaard FJ, Haasbeek CJ, et al. Patterns of disease recurrence after stereotactic ablative radiotherapy for early stage non-small-cell lung cancer: a retrospective analysis. Lancet Oncol 2012;13:802-9.
10. Sun B, Brooks ED, Komaki RU, et al. 7-year follow-up after stereotactic ablative radiotherapy for patients with stage I non-small cell lung cancer: Results of a phase 2 clinical trial. Cancer 2017;123:3031-9.
11. Baumann P, Nyman J, Hoyer M, et al. Outcome in a prospective phase II trial of medically inoperable stage I non-small-cell lung cancer patients treated with stereotactic body radiotherapy. J Clin Oncol 2009;27:3290-6.
12. Dunlap NE, Larner JM, Read PW, et al. Size matters: a

comparison of T1 and T2 peripheral non-small-cell lung cancers treated with stereotactic body radiation therapy (SBRT). J Thorac Cardiovasc Surg 2010;140:583-9.
13. Baumann P, Nyman J, Lax I, et al. Factors important for efficacy of stereotactic body radiotherapy of medically inoperable stage I lung cancer. A retrospective analysis of patients treated in the Nordic countries. Acta Oncol 2006;45:787-95.
14. Parker SM, Siochi RA, Wen S, et al. Impact of Tumor Size on Local Control and Pneumonitis After Stereotactic Body Radiation Therapy for Lung Tumors. Pract Radiat Oncol 2019;9:e90-7.
15. Zhao L, Zhou S, Balter P, et al. Planning Target Volume D95 and Mean Dose Should Be Considered for Optimal Local Control for Stereotactic Ablative Radiation Therapy. Int J Radiat Oncol Biol Phys 2016;95:1226-35.
16. Woody NM, Stephans KL, Andrews M, et al. A Histologic Basis for the Efficacy of SBRT to the lung. J Thorac Oncol 2017;12:510-9.
17. Baine MJ, Verma V, Schonewolf CA, et al. Histology significantly affects recurrence and survival following SBRT for early stage non-small cell lung cancer. Lung Cancer 2018;118:20-6.
18. Kohutek ZA, Wu AJ, Zhang Z, et al. FDG-PET maximum standardized uptake value is prognostic for recurrence and survival after stereotactic body radiotherapy for non-small cell lung cancer. Lung Cancer 2015;89:115-20.
19. Takeda A, Yokosuka N, Ohashi T, et al. The maximum standardized uptake value (SUVmax) on FDG-PET is a strong predictor of local recurrence for localized non-small-cell lung cancer after stereotactic body radiotherapy (SBRT). Radiother Oncol 2011;101:291-7.
20. Bollineni VR, Widder J, Pruim J, et al. Residual (1)(8) F-FDG-PET uptake 12 weeks after stereotactic ablative radiotherapy for stage I non-small-cell lung cancer predicts local control. Int J Radiat Oncol Biol Phys 2012;83:e551-5.
21. Onishi H, Shirato H, Nagata Y, et al. Hypofractionated stereotactic radiotherapy (HypoFXSRT) for stage I non-small cell lung cancer: updated results of 257 patients in a Japanese multi-institutional study. J Thorac Oncol 2007;2:S94-100.
22. Kestin L, Grills I, Guckenberger M, et al. Dose-response relationship with clinical outcome for lung stereotactic body radiotherapy (SBRT) delivered via online image guidance. Radiother Oncol 2014;110:499-504.
23. Latifi K, Oliver J, Baker R, et al. Study of 201 non-small cell lung cancer patients given stereotactic ablative radiation therapy shows local control dependence on dose calculation algorithm. Int J Radiat Oncol Biol Phys 2014;88:1108-13.
24. Ye L, Shi S, Zeng Z, et al. Nomograms for predicting disease progression in patients of Stage I non-small cell lung cancer treated with stereotactic body radiotherapy. Jpn J Clin Oncol 2018;48:160-6.
25. Shiue K, Cerra-Franco A, Shapiro R, et al. Histology, Tumor Volume, and Radiation Dose Predict Outcomes in NSCLC Patients After Stereotactic Ablative Radiotherapy. J Thorac Oncol 2018;13:1549-59.
26. Loganadane G, Martinetti F, Mercier O, et al. Stereotactic ablative radiotherapy for early stage non-small cell lung cancer: A critical literature review of predictive factors of relapse. Cancer Treat Rev 2016;50:240-6.
27. Spratt DE, Wu AJ, Adeseye V, et al. Recurrence Patterns and Second Primary Lung Cancers After Stereotactic Body Radiation Therapy for Early-Stage Non-Small-Cell Lung Cancer: Implications for Surveillance. Clin Lung Cancer 2016;17:177-183.e2.
28. Huang K, Dahele M, Senan S, et al. Radiographic changes after lung stereotactic ablative radiotherapy (SABR)--can we distinguish recurrence from fibrosis? A systematic review of the literature. Radiother Oncol 2012;102:335-42.
29. Dahele M, Palma D, Lagerwaard F, et al. Radiological changes after stereotactic radiotherapy for stage I lung cancer. J Thorac Oncol 2011;6:1221-8.
30. Marks LB, Bentzen SM, Deasy JO, et al. Radiation dose-volume effects in the lung. Int J Radiat Oncol Biol Phys 2010;76:S70-6.
31. Choi YW, Munden RF, Erasmus JJ, et al. Effects of radiation therapy on the lung: radiologic appearances and differential diagnosis. Radiographics 2004;24:985-97; discussion 998.
32. Yirmibesoglu E, Higginson DS, Fayda M, et al. Challenges scoring radiation pneumonitis in patients irradiated for lung cancer. Lung Cancer 2012;76:350-3.
33. Zhao J, Yorke ED, Li L, et al. Simple Factors Associated With Radiation-Induced Lung Toxicity After Stereotactic Body Radiation Therapy of the Thorax: A Pooled Analysis of 88 Studies. Int J Radiat Oncol Biol Phys 2016;95:1357-66.
34. Tekatli H, van 't Hof S, Nossent EJ, et al. Use of Stereotactic Ablative Radiotherapy (SABR) in Non-Small Cell Lung Cancer Measuring More Than 5 cm. J Thorac Oncol 2017;12:974-82.
35. Ong CL, Palma D, Verbakel WF, et al. Treatment of large stage I-II lung tumors using stereotactic body radiotherapy

(SBRT): planning considerations and early toxicity. Radiother Oncol 2010;97:431-6.
36. Chen H, Senan S, Nossent EJ, et al. Treatment-Related Toxicity in Patients With Early-Stage Non-Small Cell Lung Cancer and Coexisting Interstitial Lung Disease: A Systematic Review. Int J Radiat Oncol Biol Phys 2017;98:622-31.
37. Palma DA, van Sornsen de Koste J, Verbakel WF, et al. Lung density changes after stereotactic radiotherapy: a quantitative analysis in 50 patients. Int J Radiat Oncol Biol Phys 2011;81:974-8.
38. Bahig H, Filion E, Vu T, et al. Severe radiation pneumonitis after lung stereotactic ablative radiation therapy in patients with interstitial lung disease. Pract Radiat Oncol 2016;6:367-74.
39. Yamaguchi S, Ohguri T, Matsuki Y, et al. Radiotherapy for thoracic tumors: association between subclinical interstitial lung disease and fatal radiation pneumonitis. Int J Clin Oncol 2015;20:45-52.
40. Yamashita H, Kobayashi-Shibata S, Terahara A, et al. Prescreening based on the presence of CT-scan abnormalities and biomarkers (KL-6 and SP-D) may reduce severe radiation pneumonitis after stereotactic radiotherapy. Radiat Oncol 2010;5:32.
41. Allibhai Z, Taremi M, Bezjak A, et al. The impact of tumor size on outcomes after stereotactic body radiation therapy for medically inoperable early-stage non-small cell lung cancer. Int J Radiat Oncol Biol Phys 2013;87:1064-70.
42. Liu H, Zhang X, Vinogradskiy YY, et al. Predicting radiation pneumonitis after stereotactic ablative radiation therapy in patients previously treated with conventional thoracic radiation therapy. Int J Radiat Oncol Biol Phys 2012;84:1017-23.
43. Kong FM, Wang S. Nondosimetric risk factors for radiation-induced lung toxicity. Semin Radiat Oncol 2015;25:100-9.
44. Okubo M, Itonaga T, Saito T, et al. Predicting risk factors for radiation pneumonitis after stereotactic body radiation therapy for primary or metastatic lung tumours. Br J Radiol 2017;90:20160508.
45. Singhvi M, Lee P. Illustrative cases of false positive biopsies after stereotactic body radiation therapy for lung cancer based on abnormal FDG-PET-CT imaging. BMJ Case Rep 2013;2013. doi: 10.1136/bcr-2012-007967.
46. Trovo M, Linda A, El Naqa I, et al. Early and late lung radiographic injury following stereotactic body radiation therapy (SBRT). Lung Cancer 2010;69:77-85.
47. Palma DA, Senan S, Haasbeek CJ, et al. Radiological and clinical pneumonitis after stereotactic lung radiotherapy: a matched analysis of three-dimensional conformal and volumetric-modulated arc therapy techniques. Int J Radiat Oncol Biol Phys 2011;80:506-13.
48. Senthi S, Dahele M, van de Ven PM, et al. Late radiologic changes after stereotactic ablative radiotherapy for early stage lung cancer: a comparison of fixed-beam versus arc delivery techniques. Radiother Oncol 2013;109:77-81.
49. Matsuo Y, Nagata Y, Mizowaki T, et al. Evaluation of mass-like consolidation after stereotactic body radiation therapy for lung tumors. Int J Clin Oncol 2007;12:356-62.
50. Takeda A, Kunieda E, Takeda T, et al. Possible misinterpretation of demarcated solid patterns of radiation fibrosis on CT scans as tumor recurrence in patients receiving hypofractionated stereotactic radiotherapy for lung cancer. Int J Radiat Oncol Biol Phys 2008;70:1057-65.
51. Linda A, Trovo M, Bradley JD. Radiation injury of the lung after stereotactic body radiation therapy (SBRT) for lung cancer: a timeline and pattern of CT changes. Eur J Radiol 2011;79:147-54.
52. Park KJ, Chung JY, Chun MS, et al. Radiation-induced lung disease and the impact of radiation methods on imaging features. Radiographics 2000;20:83-98.
53. Chen F, Matsuo Y, Yoshizawa A, et al. Salvage lung resection for non-small cell lung cancer after stereotactic body radiotherapy in initially operable patients. J Thorac Oncol 2010;5:1999-2002.
54. Hamaji M, Chen F, Matsuo Y, et al. Treatment and Prognosis of Isolated Local Relapse after Stereotactic Body Radiotherapy for Clinical Stage I Non-Small-Cell Lung Cancer: Importance of Salvage Surgery. J Thorac Oncol 2015;10:1616-24.
55. Taira N, Kawabata T, Ichi T, et al. Salvage operation for late recurrence after stereotactic body radiotherapy for lung cancer: two patients with no viable cancer cells. Ann Thorac Surg 2014;97:2167-71.
56. Stauder MC, Rooney JW, Neben-Wittich MA, et al. Late tumor pseudoprogression followed by complete remission after lung stereotactic ablative radiotherapy. Radiat Oncol 2013;8:167.
57. Eisenhauer EA, Therasse P, Bogaerts J, et al. New response evaluation criteria in solid tumours: revised RECIST guideline (version 1.1). Eur J Cancer 2009;45:228-47.
58. Mattonen SA, Palma DA, Haasbeek CJ, et al. Distinguishing radiation fibrosis from tumour recurrence after stereotactic ablative radiotherapy (SABR) for lung cancer: a quantitative analysis of CT density changes. Acta

Oncol 2013;52:910-8.
59. Mattonen SA, Palma DA, Haasbeek CJ, et al. Early prediction of tumor recurrence based on CT texture changes after stereotactic ablative radiotherapy (SABR) for lung cancer. Med Phys 2014;41:033502.
60. Mattonen SA, Palma DA, Johnson C, et al. Detection of Local Cancer Recurrence After Stereotactic Ablative Radiation Therapy for Lung Cancer: Physician Performance Versus Radiomic Assessment. Int J Radiat Oncol Biol Phys 2016;94:1121-8.
61. Huang K, Senthi S, Palma DA, et al. High-risk CT features for detection of local recurrence after stereotactic ablative radiotherapy for lung cancer. Radiother Oncol 2013;109:51-7.
62. Peulen H, Mantel F, Guckenberger M, et al. Validation of High-Risk Computed Tomography Features for Detection of Local Recurrence After Stereotactic Body Radiation Therapy for Early-Stage Non-Small Cell Lung Cancer. Int J Radiat Oncol Biol Phys 2016;96:134-41.
63. Ronden MI, van Sornsen de Koste JR, Johnson C, et al. Incidence of High-Risk Radiologic Features in Patients Without Local Recurrence After Stereotactic Ablative Radiation Therapy for Early-Stage Non-Small Cell Lung Cancer. Int J Radiat Oncol Biol Phys 2018;100:115-21.
64. Nguyen TK, Senan S, Bradley JD, et al. Optimal imaging surveillance after stereotactic ablative radiation therapy for early-stage non-small cell lung cancer: Findings of an International Delphi Consensus Study. Pract Radiat Oncol 2018;8:e71-8.
65. Zhang X, Liu H, Balter P, et al. Positron emission tomography for assessing local failure after stereotactic body radiotherapy for non-small-cell lung cancer. Int J Radiat Oncol Biol Phys 2012;83:1558-65.
66. Takeda A, Kunieda E, Fujii H, et al. Evaluation for local failure by 18F-FDG PET/CT in comparison with CT findings after stereotactic body radiotherapy (SBRT) for localized non-small-cell lung cancer. Lung Cancer 2013;79:248-53.
67. Essler M, Wantke J, Mayer B, et al. Positron-emission tomography CT to identify local recurrence in stage I lung cancer patients 1 year after stereotactic body radiation therapy. Strahlenther Onkol 2013;189:495-501.
68. Lovinfosse P, Janvary ZL, Coucke P, et al. FDG PET/CT texture analysis for predicting the outcome of lung cancer treated by stereotactic body radiation therapy. Eur J Nucl Med Mol Imaging 2016;43:1453-60.
69. Huang K, Dahele M, Senan S, et al. Radiographic Changes After Lung Stereotactic Ablative Radiotherapy (SABR) -- Can We Distinguish Fibrosis From Recurrence? A Systematic Review of the Literature. Pract Radiat Oncol 2013;3:S11-2.
70. Kinahan PE, Fletcher JW. Positron emission tomography-computed tomography standardized uptake values in clinical practice and assessing response to therapy. Semin Ultrasound CT MR 2010;31:496-505.
71. Matsuo Y, Nakamoto Y, Nagata Y, et al. Characterization of FDG-PET images after stereotactic body radiation therapy for lung cancer. Radiother Oncol 2010;97:200-4.
72. Song C, Hong BJ, Bok S, et al. Real-time Tumor Oxygenation Changes After Single High-dose Radiation Therapy in Orthotopic and Subcutaneous Lung Cancer in Mice: Clinical Implication for Stereotactic Ablative Radiation Therapy Schedule Optimization. Int J Radiat Oncol Biol Phys 2016;95:1022-31.
73. Miller GW, Mugler JP 3rd, Sá RC, et al. Advances in functional and structural imaging of the human lung using proton MRI. NMR Biomed 2014;27:1542-56.
74. Shintani T, Matsuo Y, Iizuka Y, et al. Assessment of treatment response after lung stereotactic body radiotherapy using diffusion weighted magnetic resonance imaging and positron emission tomography: A pilot study. Eur J Radiol 2017;92:58-63.
75. Hallac RR, Zhou H, Pidikiti R, et al. A role for dynamic contrast-enhanced magnetic resonance imaging in predicting tumour radiation response. Br J Cancer 2016;114:1206-11.
76. Huang YS, Chen JL, Hsu FM, et al. Response assessment of stereotactic body radiation therapy using dynamic contrast-enhanced integrated MR-PET in non-small cell lung cancer patients. J Magn Reson Imaging 2018;47:191-9.
77. Jackson A, O'Connor JP, Parker GJ, et al. Imaging tumor vascular heterogeneity and angiogenesis using dynamic contrast-enhanced magnetic resonance imaging. Clin Cancer Res 2007;13:3449-59.
78. de Langen AJ, van den Boogaart V, Lubberink M, et al. Monitoring response to antiangiogenic therapy in non-small cell lung cancer using imaging markers derived from PET and dynamic contrast-enhanced MRI. J Nucl Med 2011;52:48-55.
79. Park HJ, Griffin RJ, Hui S, et al. Radiation-induced vascular damage in tumors: implications of vascular damage in ablative hypofractionated radiotherapy (SBRT and SRS). Radiat Res 2012;177:311-27.
80. Lambin P, Rios-Velazquez E, Leijenaar R, et al. Radiomics: extracting more information from medical images using

advanced feature analysis. Eur J Cancer 2012;48:441-6.
81. Huynh E, Coroller TP, Narayan V, et al. Associations of Radiomic Data Extracted from Static and Respiratory-Gated CT Scans with Disease Recurrence in Lung Cancer Patients Treated with SBRT. PloS One 2017;12:e0169172.
82. Aerts HJ, Velazquez ER, Leijenaar RT, et al. Decoding tumour phenotype by noninvasive imaging using a quantitative radiomics approach. Nat Commun 2014;5:4006. Erratum in: Nat Commun 2014;5:4644. Cavalho, Sara [corrected to Carvalho, Sara].
83. Defraene G, van Elmpt W, Crijns W, et al. CT characteristics allow identification of patient-specific susceptibility for radiation-induced lung damage. Radiother Oncol 2015;117:29-35.
84. Ghobadi G, Wiegman EM, Langendijk JA, et al. A new CT-based method to quantify radiation-induced lung damage in patients. Radiother Oncol 2015;117:4-8.
85. Cunliffe A, Armato SG 3rd, Castillo R, et al. Lung texture in serial thoracic computed tomography scans: correlation of radiomics-based features with radiation therapy dose and radiation pneumonitis development. Int J Radiat Oncol Biol Phys 2015;91:1048-56.
86. Fave X, Zhang L, Yang J, et al. Delta-radiomics features for the prediction of patient outcomes in non-small cell lung cancer. Sci Rep 2017;7:588.
87. Ettinger DS, Wood DE, Aisner DL, et al. Non-Small Cell Lung Cancer, Version 5.2017, NCCN Clinical Practice Guidelines in Oncology. J Natl Compr Canc Netw 2017;15:504-35.
88. Jaklitsch MT, Jacobson FL, Austin JH, et al. The American Association for Thoracic Surgery guidelines for lung cancer screening using low-dose computed tomography scans for lung cancer survivors and other high-risk groups. J Thorac Cardiovasc Surg 2012;144:33-8.
89. Zhang J, Yang F, Li B, et al. Which is the optimal biologically effective dose of stereotactic body radiotherapy for Stage I non-small-cell lung cancer? A meta-analysis. Int J Radiat Oncol Biol Phys 2011;81:e305-16.

doi: 10.21037/tro.2019.03.05
Cite this article as: Mathieu D, Bahig H. Response assessment and surveillance following stereotactic ablative radiotherapy for lung cancer. Ther Radiol Oncol 2019;3:15.

